Received: 20 April 2022 | Accepted: 9 June 2022

DOI: 10.1111/1759-7714.14550

ORIGINAL ARTICLE

WILEY

A novel circ_0000654/miR-375/E2F3 ceRNA network in esophageal squamous cell carcinoma

Chunyu Luo | **Xiaowei Zhao** | **Yuan Wang** | **Yanqiu Li** | **Tuo Wang** | **Shumin Li**

Department of Clinical Laboratory, Affiliated Hospital of Chifeng University, Chifeng, China

Correspondence
Shumin Li, Department of Clinical Laboratory, Affiliated Hospital of Chifeng University, No. 42, Wangfu Street, Xincheng, Songshan District, Chifeng 024005, China.
Email: lishumin8407@163.com

Abstract

Background: The competing endogenous RNA (ceRNA) activity of circular RNAs (circRNAs) has been implicated in the pathogenesis of cancers, including esophageal squamous cell carcinoma (ESCC). Here, we identified the ceRNA mechanism of circ_0000654 regulation in ESCC.

Methods: The levels of circ_0000654, E2F transcription factor 3 (E2F3), and microRNA (miR)-375 were gauged by quantitative real-time PCR (qRT-PCR) and western blot. Cell proliferation was assessed by 3-(4,5-dimethylthiazol-2-yl)-5-(3-carboxymethoxyphenyl)-2-(4-sulfophenyl)-2H-tetrazolium (MTS) and 5-ethynyl-2′-deoxyuridine (EdU) assays. Cell apoptosis was detected by flow cytometry. Cell colony formation was tested by colony formation assay. Dual-luciferase reporter, RNA pull-down and RNA immunoprecipitation (RIP) assays were performed to confirm the direct relationship between miR-375 and circ_0000654 or E2F3. Xenograft model assays were used to evaluate the effect of circ_0000654 in vivo.

Results: Circ_0000654 and E2F3 were upregulated in ESCC. Circ_0000654 depletion enhanced cell apoptosis and hindered cell proliferation and glycolysis in vitro, as well as weakened tumor growth in vivo. Increased expression of E2F3 counteracted the effects of circ_0000654 depletion. Mechanistically, E2F3 was a target of miR-375, and circ_0000654 modulated E2F3 expression through sequestering miR-375. Furthermore, miR-375 upregulation phenocopied circ_0000654 knockdown in inhibiting ESCC progression.

Conclusion: Our findings identify a new circ_0000654/miR-375/E2F3 ceRNA crosstalk for the oncogenic role of circ_0000654 in ESCC and establish a notion that targeting circ_0000654 and its pathways may have the potential to improve ESCC outcome.

KEYWORDS
ceRNA crosstalk, circ_0000654, E2F transcription factor 3 (E2F3), ESCC, miR-375

INTRODUCTION

Worldwide, esophageal squamous cell carcinoma (ESCC) is one of the most commonly occurring malignancies, with a high mortality because of advanced stage at diagnosis.[1] Despite advances in diagnostic and therapeutic regimens, the curative treatments of advanced ESCC, defined as metastatic or recurrent ESCC, remain limited.[2,3] Essential regulators of the pathogenesis of ESCC, including circular RNAs (circRNAs) and proteins, are under intensive study.[4–7] A more thorough understanding of the roles of these regulatory molecules in ESCC may lead to therapeutic breakthroughs in further personalized medicine.

Unlike linear RNAs, covalently closed circRNAs are natural RNA circles with neither 5′-3′ polarities nor poly (A) tails.[8] Numerous circRNAs, generated by head-to-tail splicing of exons, possess an important regulatory potential of coding sequences.[9] Recent research has documented the competing endogenous RNA (ceRNA) activity of some circRNAs through microRNAs (miRNAs), highlighting the

implications of these ceRNA networks in human cancers, including ESCC.[10–12] For example, Shi et al. uncovered that circ_0006168 operated as a potent oncogenic driver in ESCC via upregulating mammalian target of rapamycin (mTOR) by sequestering miR-100.[13] Pan et al. demonstrated that circ_0006948 worked as a ceRNA for miR-490-3p to contribute to ESCC progression depending on the modulation of high-mobility group AT-hook 2.[14] As for circ_0000654, formed by back-splicing of exons of chromodomain helicase DNA binding protein 2 mRNA, has been discovered to involve in the pathogenesis of ESCC.[15] Although the findings reported by Xu and colleagues have identified the miR-149-5p/interleukin 6 (IL-6) axis in the regulation of circ_0000654,[15] our understanding of its ceRNA activity in ESCC has remained fragmentary.

E2F transcription factor 3 (E2F3), a member of E2F transcription factor family that controls DNA synthesis, cell cycle, and cell death, has been underscored as a strong oncogene in numerous tumors.[16–19] Moreover, E2F3 is involved in the carcinogenic mechanism of ESCC.[20–22] Furthermore, it is still undefined whether E2F3 can work as a downstream effector of circ_0000654 in regulating ESCC development.

miRNAs lead to post-transcriptional gene silencing in a sequence-specific manner, and aberrant expression is accepted to be associated with the pathogenesis of cancers, including ESCC.[23,24] miR-375 has been suggested to be a promising prognostic biomarker for ESCC,[25,26] and it can function as a potential antitumor factor in ESCC.[27,28] Here we studied the mechanism of circ_0000654 function in ESCC and identified a novel circ_0000654/miR-375/E2F3 ceRNA network in ESCC pathogenesis.

MATERIALS AND METHODS

Human clinical specimens

This study was approved by the Ethics Committee of the Affiliated Hospital of Chifeng University and was carried out according to the guidelines of Declaration of Helsinki. We collected human specimens (including ESCC specimens, matched normal esophageal tissues, and serum samples) from 44 ESCC patients with available clinical data and confirmed diagnosis by two pathologists at the Affiliated Hospital of Chifeng University. As controls, we harvested serum specimens from 28 healthy donors without known illnesses and medications. We obtained these specimens with written informed consent provided by all patients and checked for circ_0000654, E2F3, and miR-375 expression by quantitative real-time PCR (qRT-PCR) or western blot as below.

Cell lines

TE-1, ECA-109, and KYSE-450 ESCC cells (Bnbio) were propagated under standard conditions provided by Bnbio. Human esophageal epithelial HET-1A cell line (Bnbio) was applied as a control and the medium employed was the bronchial epithelial cell growth medium (BEGM) from Lonza. We maintained all cells at 37°C in a 5% CO_2 incubator.

Preparation of total RNA and protein

We extracted total RNA and protein using the AllPrep DNA/RNA/Protein Mini Kit from collected tissues and cultured cells based on the manufacturer's guidance (Qiagen). For analysis of protein concentration, the Bradford protein assay was employed with the available kit (Leagene). For analysis of RNA purity and quantify, a NanoVue Spectrum photometer was used as per the manufacturing protocols (GE Healthcare). We prepared nuclear and cytoplasmic RNA from TE-1 and ECA-109 cells using the Cytoplasmic & Nuclear RNA Purification Kit as described by the manufacturers (Norgen).

qRT-PCR

For cDNA preparation, RNA was reverse-transcribed by M-MLV reverse transcriptase (Promega) with a random hexamer (for circ_0000654), oligo(dT) primer (for mRNA), and a stem-loop RT primer (for miR-375), purchased from TaKaRa. qRT-PCR was done on the Light Cycler 480 II (Roche) with a master mix of diluted cDNA, SYBR Green (TaKaRa), and specific primer pairs (shown in Table S1). Using the $2^{-\Delta\Delta Ct}$ formula,[29] expression of targets was evaluated relative to the housekeeping gene β-actin (for circ_0000654 and mRNA) or U6 (for miR-375).

Western blot

After equal amounts (30 μg) of protein were separated on NuPAGE Novex 4%–12% gels (Thermo Fisher Scientific), the resulting gels were electroblotted onto nitrocellulose membranes (GE Healthcare). For immunoblotting, we used anti-E2F3 (Cat#PA5-114490; Life Technologies), anti-c-Myc (Cat#PA5-85185; Life Technologies), anti-BCL-2 (Cat#PA5-20068; Life Technologies), and anti-β-actin (Cat#ab8227; Abcam) primary antibodies and goat anti-rabbit IgG secondary antibody (Cat#G-21234; Life Technologies) before addition of a chemiluminescent substrate (Thermo Fisher Scientific).

Circ_0000654 depletion by RNA interference

We silenced circ_0000654 in ESCC cells by transiently transfecting targeted shRNA plasmid (sh-circ_0000654, for in vitro assays) or by transducing cells with shRNA-expressing lentiviral constructs (sh-circ_0000654, for in vivo studies). For transient transfection, sh-circ_0000654 (Geneseed) and a nonsilencing shRNA (sh-circ_NC) were used. TE-1 and ECA-109 cells were plated in 12-well dishes (1×10^5 per well) in growth medium with antibiotics. The second day, a mix of shRNA (50 nM), oligofectamine

reagent, and Opti-MEMI medium was prepared as recommended by the manufacturers (Life Technologies) and dispensed in each well. We harvested the cells after 48 h for further in vitro experiments. For stable transduction, puromycin-selectable lentiviral particles expressing sh-circ_0000654 or shRNA control (sh-circ_NC), provided by Geneseed, were used to transduce ECA-109 cells in growth medium plus polybrene (8 μg/ml; MKBio). We selected virus-transduced cells with puromycin (2 μg/ml, MKBio) for over 2 weeks for in vivo studies.

Generation of miR-375 or E2F3 overexpressing and knockdown cells

Human E2F3 (Accession: NM_001243076.3) coding sequence and a scrambled control sequence, provided by GeneCreate, were incubated with BamH I and Xho I endonucleases and cloned in the pcDNA3.1 vector (WZ Biosciences Inc.), respectively. The plasmid construct expressing miRNA inhibitor (in-miR-375, 5′-UCACGCGAGCCGAACGAACAAA-3′; Ribobio) was designed to knock down miR-375. As the control, a nontargeting plasmid expressing in-miR-NC was used. The miR-375 mimic (5′-UUUGUUCGUUCGGCUCGCGUGA-3′; Ribobio) was the mature miRNA sequence, and miR-NC mimic control mock (Ribobio) was the control. For in vitro E2F3 upregulation assays, TE-1 and ECA-109 cells were transfected using Fugene with plasmid construct (200 ng) as per the manufacturing instructions (Promega). For in vitro miR-375 reduction experiments, TE-1 and ECA-109 cells were transiently transfected with 30 nM of miRNA mimic using oligofectamine reagent (Life Technologies). We harvested the transfected cells and performed further assays after 48 h.

Cell proliferation assay

Transfected TE-1 and ECA-109 cells were seeded into 96-well dishes (∼2000 cells per well) before incubating at 37°C for the desired duration. Evaluation of cell proliferation was conducted under the usage of the 3-(4,5-dimethylthiazol-2-yl)-5-(3-carboxymethoxyphenyl)-2-(4-sulfophenyl)-2H-tetrazolium (MTS) assay with CellTiter96 AQueous One Solution (Promega) and 5-ethynyl-2′-deoxyuridine (EdU) assay with the EdU Apollo567 Kit (Ribobio) as per the accompanying recommendations. For proliferation determination, we measured the absorbance with a plate reader (iMark, Bio-Rad 680) at 490 nM and read EdU-positive $^{(+)}$ cells under fluorescence microscopy (Olympus).

Cell apoptosis assay

Transfected TE-1 and ECA-109 cells were incubated with propidium iodide (PI) and fluorescein isothiocyanate (FITC)-Annexin V as recommended by the Apoptosis Assay Kit (Solarbio) and analyzed within 1 h. We defined the apoptotic cells as the population that was positive for Annexin V.

Cell colony formation assay

Transfected TE-1 and ECA-109 cells (200 cells/well) were grown in six-well culture dishes at 5% CO_2 at 37°C. Following 10–14 days of incubation, the colonies (≥50 cells) were assessed after staining by crystal violet (0.5%).

Determination of glucose uptake and lactate production levels

We determined glucose uptake level using the Glucose Uptake Assay Kit and lactate production level with Lactate Assay Kit as per the manufacturing guidelines (Abcam).

Bioinformatics

The miRNA-pairing sites to circ_0000654 were searched using the CircInteractome online web (https://circinteractome.nia.nih.gov/). The molecular target mRNAs of miR-375 were downloaded from the ENCORI computer algorithm (http://starbase.sysu.edu.cn/) based on the presence of a 3' untranslated region (3'UTR).

Dual-luciferase reporter assay

The segments of circ_0000654 and E2F3 3'UTR encompassing the predicted miR-375 complementary sites or mismatched pairing sequences (GAACAA was mutated to CUUGUU), obtained from GeneCreate, were cloned into the appropriate sites of the pMIR-REPORT vector (Life Technologies). About 1×10^5 TE-1 and ECA-109 cells were co-transfected using Lipofectamine 3000 (Life Technologies) with 100 ng of the indicated firefly reporter construct, 20 ng of pRL-TK Renilla luciferase normalization control (Promega), and 30 nM of miRNA mimic. Thirty-six hours later, cells were processed using the Dual-luciferase Reporter Assay System from Promega.

RNA pull-down and (RIP) assays

We prepared the lysates of TE-1 and ECA-109 cells under the use of the RIPA lysis buffer (Solarbio). For RNA pull-down experiments, we incubated cell lysates with streptavidin magnetic beads (Life Technologies) previously coated with biotinylated miR-375 mimic (Bio-miR-375), biotinylated miR-346 mimic (Bio-miR-346) or Bio-NC mock (all from Ribobio). For RNA immunoprecipitation (RIP) experiments, we exposed cell lysates to Protein A/G Agarose (Life Technologies) previously coated with either anti-Ago2 (Cat#ab233727) or anti-IgG (Cat#ab172730) antibody (Abcam). Following a 6-h incubation at 4°C, RNA bound to beads was processed by qRT-PCR to quantify circ_0000654 and E2F3 mRNA enrichment levels.

Xenograft model assays

All research involving animals complied with international guidelines and protocols approved by the Ethics Committee on Animal Care and Use of Affiliated Hospital of Chifeng University. For xenograft model studies, female Balb/c nude mice age-matched between 6 and 8 weeks (Beijing Vital River Laboratory Animal Technology Co., Ltd) were implanted with 2×10^6 sh-circ_0000654- or sh-NC-transduced ECA-109 cells (resuspended in 200 μl phosphate buffered saline) via subcutaneous injection (six mice each group). Tumor volume was periodically monitored by a digital caliper and evaluated by the $0.5 \times \text{length} \times \text{width}^2$ formula. Xenograft tumors were harvested and weighed after 28 days. Fresh tumor tissues were used to quantify circ_0000654 and miR-375 expression by qRT-PCR. Paraffin-embedded tumor tissues were processed by immunohistochemistry analysis using anti-BCL-2 (Cat#PA5-20068), anti-c-Myc (Cat#PA5-85185), and anti-E2F3 (Cat#PA5-106407, all from Life Technologies) antibodies under standard protocols.[30]

Statistical analysis

Unless otherwise noted, a Student's *t*-test (two-tailed) or analysis for variance was used for comparisons. The difference of gene expression in human clinical specimens was analyzed by the Mann–Whitney U-test. All experiments were done with at least three biological replicates. Error bars represented the standard deviation. $p < 0.05$ indicated significant difference. RNA expression correlations in clinical specimens were analyzed by Pearson's correlation coefficients.

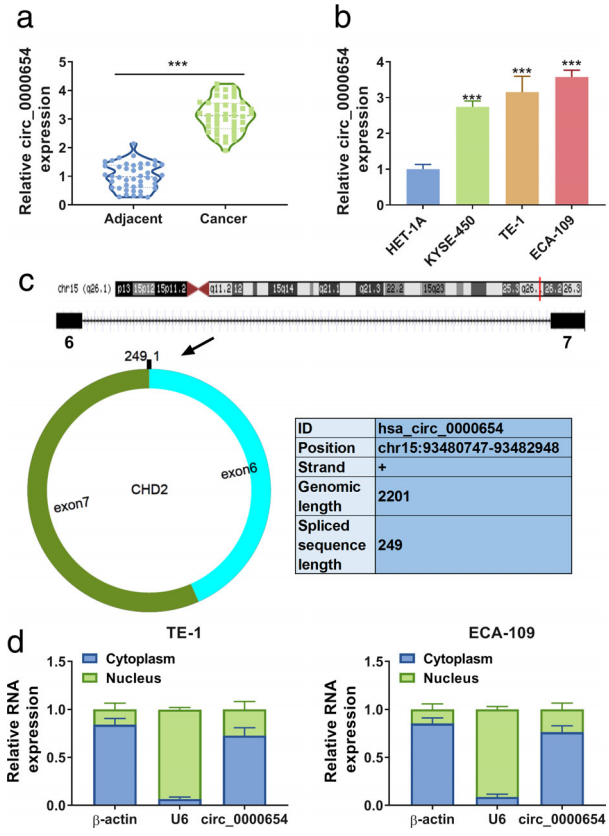

FIGURE 1 Circ_0000654 is upregulated in ESCC tissues and cells. (a) qRT-PCR analysis of circ_0000654 in paired normal and cancer tissues from the same cohorts ($n = 44$). (b) qRT-PCR analysis showing circ_0000654 expression in HET-1A, KYSE-450, TE-1, and ECA-109 cells. (c) Schematic model of circ_0000654 formation by back-splicing of exons 6 and 7 of CHD2. (d) Subcellular fractionation assay showing the localization of circ_0000654 in TE-1 and ECA-109 cells. ***$p < 0.001$

RESULTS

Overexpression of circ_0000654 in human ESCC

To validate circ_0000654 deregulation in relation to the development of ESCC, we first performed the expression analysis on matched tumor and normal tissues from 44 patients with primary ESCC. Indeed, circ_0000654 expression was clearly elevated in tumor tissues compared with the controls (Figure 1A). Additionally, high expression of circ_0000654 was observed in serum samples of ESCC patients versus healthy controls (Figure S1). In line with the tumor tissues, ESCC cells exhibited higher levels of circ_0000654 compared with the normal esophageal HET-1A cells (Figure 1B). Circ_0000654 was a 249-nucleotide circular transcript generated by the back-splicing of exons 6 and 7 of CHD2 located at chromosome 15:93480747–93 482 948 (Figure 1C). Additionally, circ_0000654 was mainly present in the cytoplasm of TE-1 and ECA-109 cells, which was validated by subcellular fractionation assays (Figure 1D).

Circ_0000654 downregulation promotes cell apoptosis and impairs cell proliferation and glycolysis in vitro

Because of the overexpression of circ_0000654 in ESCC, we then examined the consequences of silencing endogenous circ_0000654. Transient transfection of shRNA plasmid targeting circ_0000654 (sh-circ_0000654) was used to reduce circ_0000654 in TE-1 and ECA-109 ESCC cells (Figure 2A), which expressed high levels of circ_0000654. Strikingly, circ_0000654 loss of function enhanced cell apoptosis (Figure 2B) and suppressed cell proliferation (Figure 2C,D) and colony formation (Figure 2E) as compared with those in the negative controls. The data of western blot revealed that silencing endogenous circ_0000654 caused a marked reduction in the expression of proliferation-related protein c-Myc and anti-apoptotic protein BCL-2 in TE-1 and ECA-109 cells (Figure 2F,G). Furthermore, downregulation of circ_0000654 led to decreased levels of glucose uptake and lactate production in TE-1 and ECA-109 cells (Figure 2H,I). Taken together, these results indicate that knockdown of

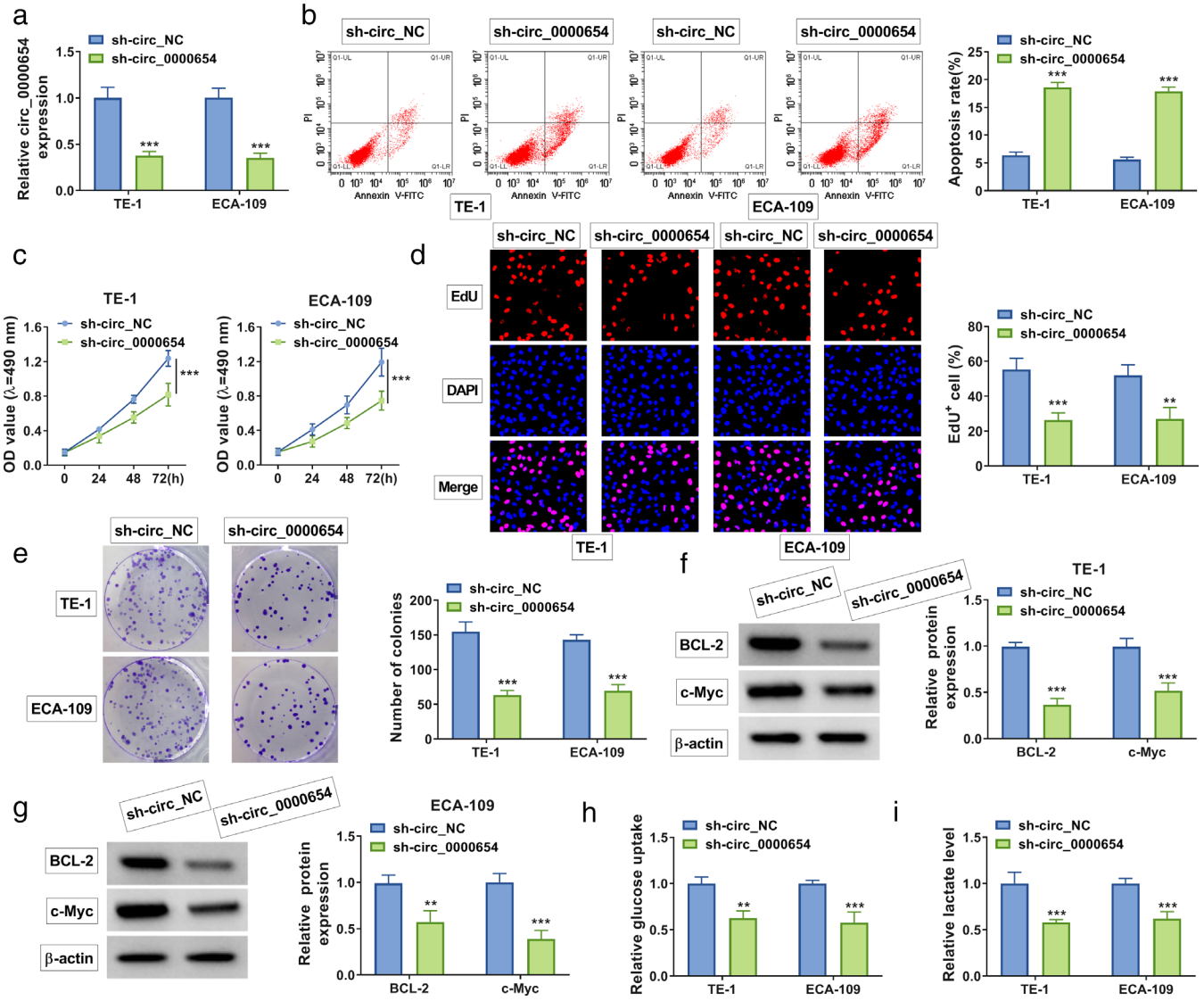

FIGURE 2 Knockdown of circ_0000654 affects cell apoptosis, proliferation, colony formation and glycolysis in vitro. (a) Relative circ_0000654 expression by qRT-PCR analysis in sh-circ_NC- or sh-circ_0000654-transfected TE-1 and ECA-109 cells. (b) Representative images showing a cell apoptosis assay and flow cytometry for apoptotic rate of sh-circ_NC- or sh-circ_0000654-transfected TE-1 and ECA-109 cells. (c) MTS assay of cell proliferation in sh-circ_NC- or sh-circ_0000654-transfected TE-1 and ECA-109 cells. (d) EdU cell proliferation assay with transfected TE-1 and ECA-109 cells. (e) Colony formation assay in TE-1 and ECA-109 cells transfected as indicated. (F and G) Western blot of BCL-2 and c-Myc protein levels in si-circ_NC- or sh-circ_0000654-transfected TE-1 and ECA-109 cells. (H and I) Levels of glucose uptake and lactate production in transfected cells using the assay kits. $^{**}p < 0.01$, $^{***}p < 0.001$

circ_0000654 promotes cell apoptosis and impedes cell proliferation and glycolysis in vitro.

Upregulation of E2F3 in human ESCC

In the meantime, we used qRT-PCR to confirm the overexpression of E2F3 oncogenic gene in ESCC tumor tissues compared with the corresponding normal controls (Figure 3A). Expression correlation analysis between circ_0000654 and E2F3 mRNA showed a positive correlation ($r = 0.534$, $p < 0.001$; Figure 3B). Our western blot data also revealed the upregulaton of E2F3 protein in ESCC tumors and cells (Figure 3C,D). Interestingly, we observed a significant reduction in the expression of E2F3 protein in TE-1 and ECA-109 cells after transfection by sh-circ_0000654 (Figure 3E). E2F3 is a functionally downstream effector of circ_0000654 in impacting cell apoptosis, proliferation, and glycolysis in vitro.

We next decided to examine whether E2F3 was a key downstream effector of circ_0000654 function. To address this possibility, we performed E2F3 restoration experiments in the presence of sh-circ_0000654. The effectiveness of E2F3 overexpression plasmid in elevating the E2F3 protein level was confirmed by western blot (Figure 4A). Restoration of E2F3 strongly abolished circ_0000654 knockdown-

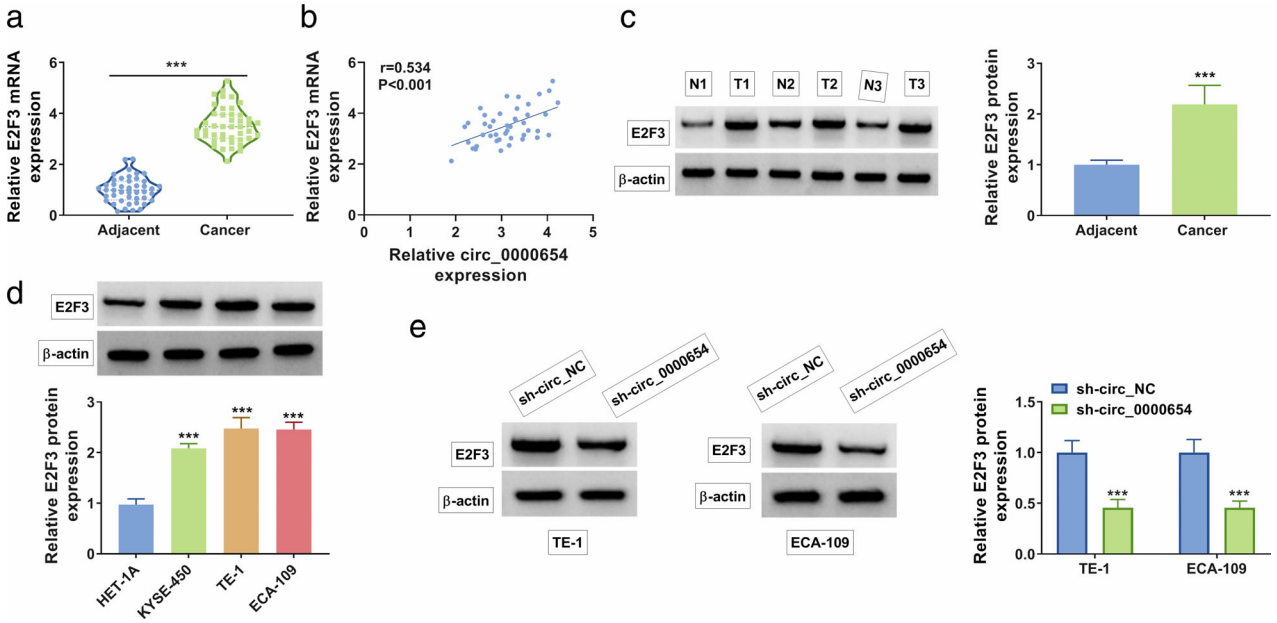

FIGURE 3 E2F3 is upregulated in human ESCC and it is regulated by circ_0000654. (a) E2F3 mRNA level by qRT-PCR analysis in matched tumor and normal tissues from the same patients with ESCC ($n = 44$). (b) Expression correlation analysis between E2F3 mRNA and circ_0000654 using Pearson's correlation coefficients. (c) E2F3 protein level by Western blot in matched tumor and normal tissues from ESCC patients ($n = 3$). (d) Western blot showing E2F3 protein level in HET-1A, KYSE-450, TE-1, and ECA-109 cells. (e) Western blot of E2F3 protein expression in TE-1 and ECA-109 cells after transfection by sh-circ_NC or sh-circ_0000654. ***$p < 0.001$

mediated apoptosis enhancement (Figure 4B), proliferation inhibition (Figure 4C,D), and colony formation reduction (Figure 4E). Restoration of E2F3 also counteracted the influence of circ_0000654 depletion on c-Myc and BCL-2 expression levels compared with the control group (Figure 4F). Additionally, E2F3 restoration partly abrogated circ_0000654 silencing-mediated inhibition of glycolysis of TE-1 and ECA-109 cells (Figure 4G,H). These findings together support our hypothesis that the effects of circ_0000654 depletion may be at least in part due to the reduction of E2F3.

Circ_0000654 regulates E2F3 expression by competitively binding to miR-375

To elucidate whether circ_0000654 could control E2F3 expression by miRNAs, we used CircInteractome online web to search miRNAs that potentially bind to circ_0000654 and used ENCORI computer algorithm to predict miRNA-binding sites based on the presence of E2F3 3'UTR. The Venn diagram revealed that there were two miRNAs (miR-375 and miR-346) predicted by both the two programs (Figure 5A). RNA pull-down assays verified that circ_0000654 and E2F3 mRNA were strongly enriched by biotinylated miR-375 mimic (Bio-miR-375), indicating the direct relationship between miR-375 and circ_0000654 or E2F3 (Figure 5B). Additionally, RIP experiments validated the association between circ_0000654 or E2F3 and the RNA-induced silencing complexes (RISCs) (Figure 5C), where miRNAs silence gene expression.[31] The miR-375 increase efficacy of miR-375 mimic transfection was ascertained by qRT-PCR (Figure 5D).

Bioinformatic analysis by CircInteractome online web predicted a putative complementary sequence for miR-375 in human circ_0000654 (Figure 5E). To verify this, we generated circ_0000654 wild-type (WT-circ_0000654) or mutant (MUT-circ_0000654) luciferase reporters and analyzed them by luciferase activity. Co-transfection of WT-circ_0000654 and miR-375 mimic into TE-1 and ECA-109 cells produced lower luciferase activity than cells co-transfected with mimic control (Figure 5F). Mutation carrying a mutated target sequence significantly abrogated the inhibition of miR-375 on reporter gene expression under the same conditions (Figure 5F). ENCORI computer algorithm predicted that the 3′UTR of E2F3 encompassed a region that matched the seed sequence of miR-375 (Figure 5G). To determine whether the altered expression of E2F3 in ESCC cells, in part, was mediated by miR-375 through its 3′UTR, we cloned the 3′UTR of E2F3 downstream of a luciferase gene as a reporter (WT-E2F3 3′UTR) and assayed it. Transfection of miR-375 mimic markedly repressed the expression of WT-E2F3 3′UTR (Figure 5H). We also generated a mutant (MUT-E2F3 3′UTR) in the seed region and found that the mutant was refractory to inhibition by miR-375 (Figure 5H), indicating that E2F3 was a direct target of miR-375. We also validated the regulation of miR-375 in E2F3 expression in TE-1 and ECA-109 cells.

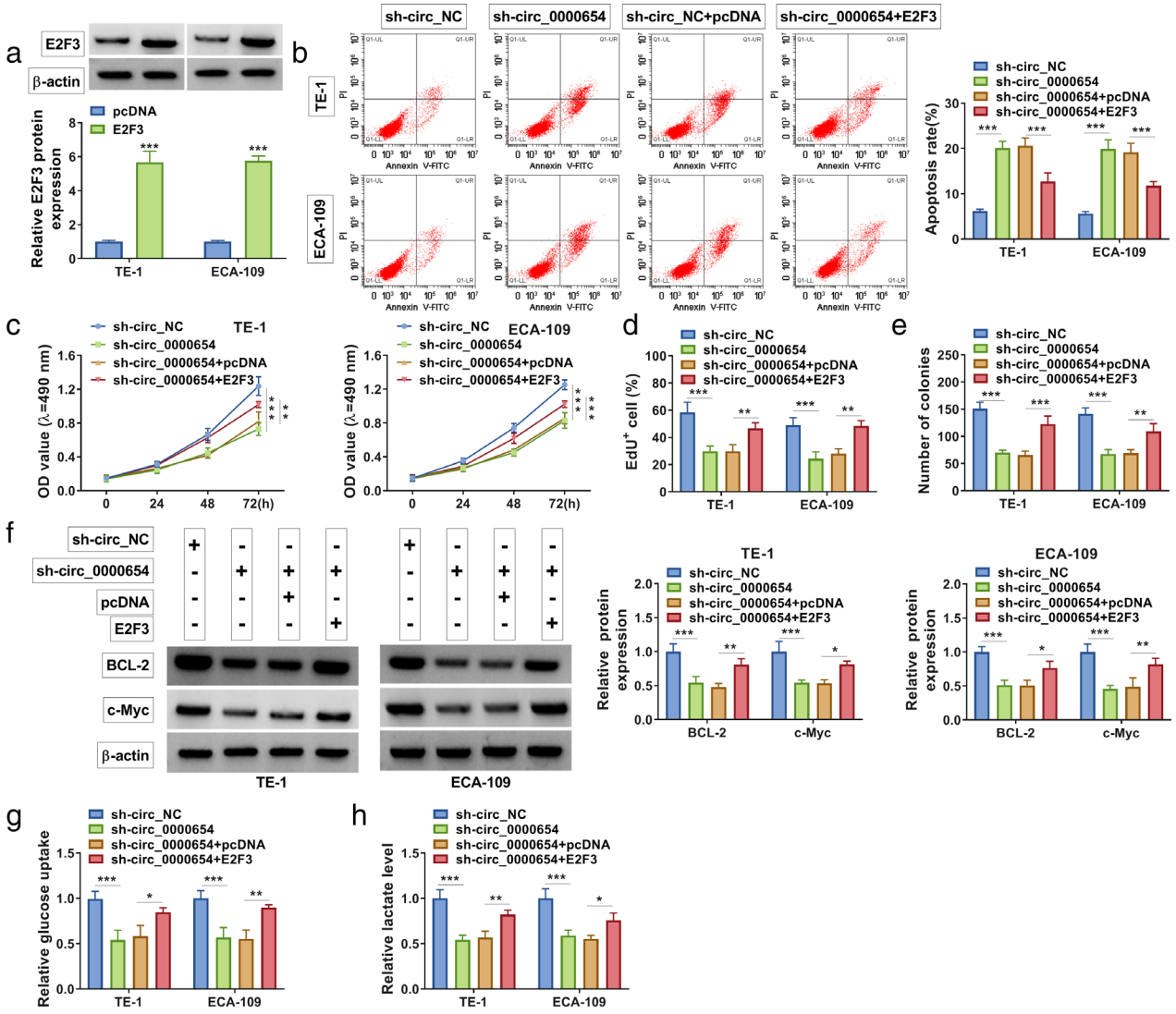

FIGURE 4 Circ_0000654 depletion affects cell apoptosis, proliferation and glycolysis by reducing E2F3. (a) Western blot analysis of E2F3 protein level in TE-1 and ECA-109 cells introduced with E2F3 overexpression plasmid (E2F3) or negative control pcDNA. (B-G) TE-1 and ECA-109 cells were transfected with sh-circ_0000654, sh-circ_NC, sh-circ_0000654 + pcDNA or sh-circ_0000654 + E2F3, followed by the evaluation of cell apoptosis by flow cytometry (b), cell proliferation by MTS and EdU assay (c and d), cell colony formation by colony formation assay (e), BCL-2 and c-Myc protein levels by western blot (f), glucose uptake and lactate production levels using the assay kits (g and h). $^{*}p < 0.05$, $^{**}p < 0.01$, $^{***}p < 0.001$

Reduction of miR-375 upon in-miR-375 transfection, verified by qRT-PCR (Figure 5I), led to an increase in E2F3 protein expression, while miR-375 overexpression inhibited E2F3 expression (Figure 5J).

We then asked whether circ_0000654 regulated E2F3 expression by operating as a ceRNA for miR-375. As expected, circ_0000654 depletion resulted in reduced expression of E2F3 protein in both TE-1 and ECA-109 cell lines, and this effect was dramatically abated by miR-375 downregulation (Figure 5K). Additionally, contrary to circ_0000654 and E2F3 levels, miR-375 was remarkably inhibited in ESCC tumor tissues (Figure 5L). Correlation analysis showed that in primary tumors, miR-375 expression inversely correlated with circ_0000654 and E2F3 mRNA levels (Figure 5M,N). Our qRT-PCR data also validated the downregulation of miR-375 in TE-1 and ECA-109 ESCC cells (Figure 5O). All these findings identify the role of circ_0000654 as a post-transcriptional regulator of E2F3 through miR-375.

MiR-375 mediates the effects of circ_0000654 on cell apoptosis, proliferation, and glycolysis in vitro.

Intriguingly, we observed a significant elevation in the abundance of miR-375 in circ_0000654-silenced TE-1 and ECA-109 cells (Figure 6A). To test whether the effects of circ_0000654 depletion were mediated by miR-375, we carried out miRNA inhibition experiments in TE-1 and ECA-109 cells transfected by sh-circ_0000654. Transfection of in-miR-375 strikingly abated circ_0000654 knockdown-mediated enhancement of miR-375 expression compared

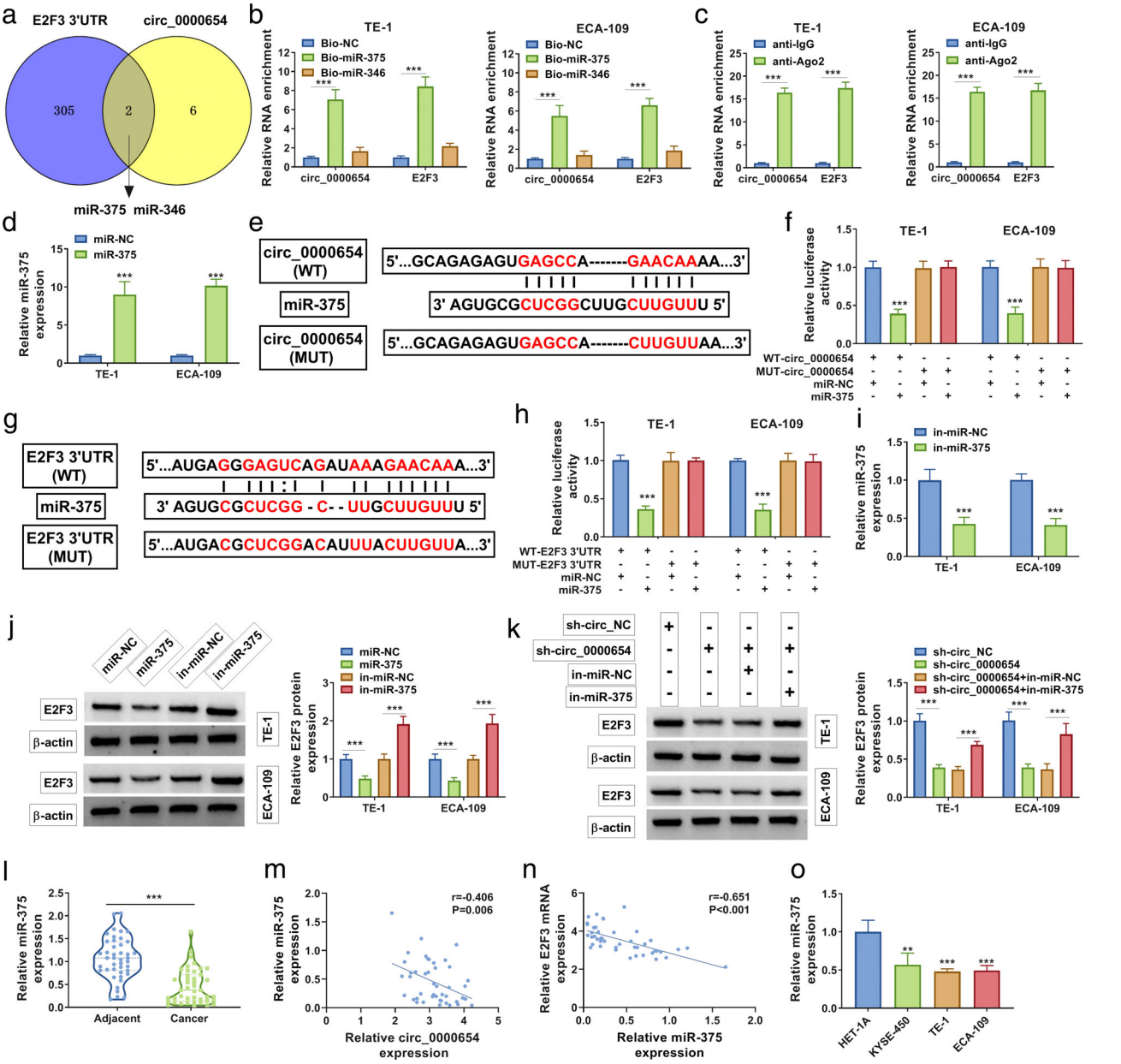

FIGURE 5 Identification of the direct relationship between miR-375 and circ_0000654 or E2F3. (a) Venn diagram showing the putative miRNAs identified by both CircInteractome and ENCORI prediction programs. (b) RNA pull-down assays on cell extracts using bio-miR-375, bio-miR-346 or bio-NC. (c) RIP experiments on cell extracts using anti-Ago2 or anti-IgG antibody. (d) qRT-PCR of miR-375 in cells after transfection by miR-375 mimic or miR-NC mimic. (e) The putative complementary sequence for miR-375 in circ_0000654, the mutation in the target sequence, and the sequence of mature miR-375. (f) Luciferase reporter assay showing the effect of miR-375 on the expression of WT-circ_0000654 and MUT-circ_0000654. (g) The predicted binding sequence for miR-375 in E2F3 3′UTR, the mutated sites in seed region, and the sequence of miR-375. (h) Luciferase reporter assay showing the effect of miR-375 on the expression of WT-E2F3 3′UTR and MUT-E2F3 3′UTR. (i) qRT-PCR of miR-375 in cells after transfection by in-miR-375 or in-miR-NC. (j) Western blot showing E2F3 protein level in cells transfected with miR-NC mimic, miR-375 mimic, in-miR-NC or in-miR-375. (k) Western blot of E2F3 protein in cells after transfection by sh-circ_0000654, sh-circ_NC, sh-circ_0000654 + pcDNA or sh-circ_0000654 + E2F3. (l) Relative miR-375 expression by qRT-PCR analysis in matched tumor and normal tissues from the same patients with ESCC ($n = 44$). (m and n) expression correlation analysis between miR-375 and circ_0000654 or E2F3 mRNA using Pearson's correlation coefficients. (o) qRT-PCR analysis of miR-375 in HET-1A, KYSE-450, TE-1, and ECA-109 cells. $^{**}p < 0.01$, $^{***}p < 0.001$

with the scrambled control (Figure 6A). Indeed, reduced expression of miR-375 clearly counteracted the pro-apoptosis (Figure 6B), anti-proliferation (Figure 6C,D), and anti-colony formation (Figure 6E) effects of circ_0000654 depletion in both TE-1 and ECA-109 cell lines. Reduced expression of miR-375 also abrogated circ_0000654 silencing-driven suppression of BCL-2 and c-Myc expression of TE-1 and ECA-109 cells (Figure 6F). Likewise, downregulation of

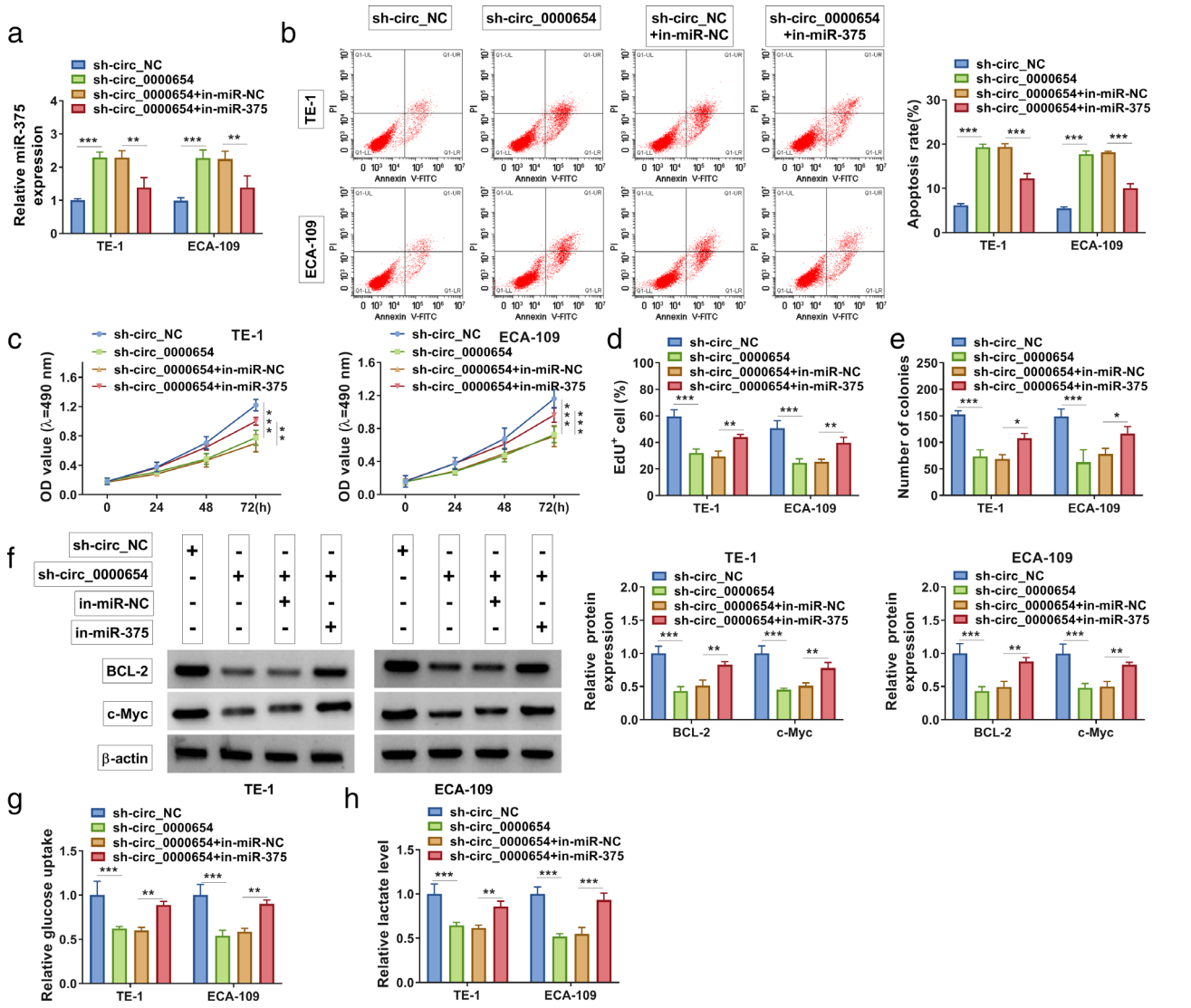

FIGURE 6 Circ_0000654 depletion affects cell apoptosis, proliferation and glycolysis in vitro by upregulating miR-375. (a–h) TE-1 and ECA-109 cells were introduced with sh-circ_0000654, sh-circ_NC, sh-circ_0000654 + in-miR-NC, or sh-circ_0000654 + in-miR-375. (a) qRT-PCR analysis of miR-375 expression in transfected TE-1 and ECA-109 cells. (b) Apoptotic rate of transfected TE-1 and ECA-109 cells by flow cytometry. (c) MTS assay for the proliferation of transfected TE-1 and ECA-109 cells. (d) EdU cell proliferation assay with transfected TE-1 and ECA-109 cells. (e) Cell colony formation using colony formation assay in transfected cells. (f) Western blot showing BCL-2 and c-Myc protein levels in transfected TE-1 and ECA-109 cells. (g and h) Glucose uptake and lactate production levels using the assay kits in transfected TE-1 and ECA-109 cells. $^{*}p < 0.05$, $^{**}p < 0.01$, $^{***}p < 0.001$

miR-375 abated circ_0000654 depletion-imposed glycolysis defect in the two cell lines (Figure 6G,H). Collectively, these data suggest that the effects of circ_0000654 depletion may be due to the elevation of miR-375.

Tumor-inhibitory effect of circ_0000654 depletion in vivo

To elucidate the role of circ_0000654 in tumor growth in vivo, we constructed stable circ_0000654-silenced ECA-109 cell line by sh-circ_0000654 lentivirus transduction and implanted the cells into the nude mice subcutaneously. Transduction of sh-circ_0000654 lentivirus significantly weakened tumor growth compared the sh-NC control (Figure 7A,B). Notably, circ_0000654 was underexpressed and miR-375 was upregulated in the sh-circ_0000654-infected ECA-109 tumors compared with the sh-NC controls (Figure 7C). Additionally, immunohistochemistry results revealed that sh-circ_0000654-infected ECA-109 tumors had fewer cells stained for E2F3, BCL-2, and c-Myc staining than sh-NC controls (Figure 7D). Taken together, these data imply that the suppression of tumor growth may be due to the reduction of circ_0000654 and E2F3 and the elevation of miR-375.

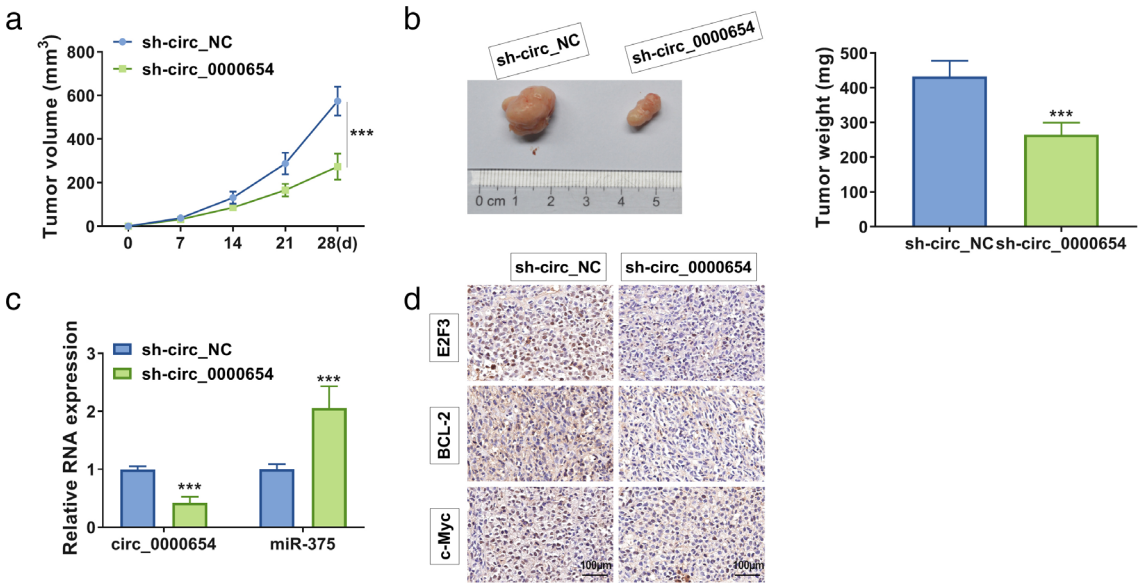

FIGURE 7 Targeting circ_0000654 affects tumor growth in vivo. (a) Growth curves of the xenograft tumors generated by subcutaneous implantation of 2×10^6 sh-circ_0000654- or sh-NC-transduced ECA-109 cells ($n = 6$ each group).Representative images and mean weight (b), qRT-PCR analysis of circ_0000654 and miR-375 (c), immunohistochemistry of E2F3, BCL-2 and c-Myc staining (d) of the xenograft tumors formed by subcutaneous implantation of 2×10^6 sh-circ_0000654- or sh-NC-transduced ECA-109 cells on day 28 after cell injection ($n = 6$ each group). $^{***}p < 0.001$

DISCUSSION

The ceRNA hypothesis proposes that circRNAs may form a crucial type of post-transcriptional modulators by operating as endogenous miRNA sponges.[32] The importance of the functional ceRNA regulation mediated by circRNAs has become increasingly clear in cancer biology.[32,33] Recent studies have illuminated that hundreds of circRNA-mediated ceRNA networks, such as ciRS-7/miR-7/Kruppel-like factor-4 and circ_0006168/miR-100/mTOR, have been implicated in ESCC pathogenesis.[10,13] Because of the oncogenic activity of circ_0000654 in ESCC,[15] we decided to explore the ceRNA mechanism of circ_0000654 function in ESCC.

E2F3 has been established as a potent oncogene in multiple types of cancers, including ESCC.[20,21] Consistent with the effect of circ_0000654 depletion, we also demonstrated that silencing endogenous E2F3 exerted a tumor suppressive activity in ESCC. Based on the suppressive effect of circ_0000654 knockdown on E2F3 protein, we first identified E2F3 as a downstream effector of circ_0000654 function in ESCC. Previous work reported that depletion of circ_0087378 inhibited E2F3 to hamper ESCC progression by competitively binding to miR-140-3p.[22]

CircRNAs and protein-coding mRNAs can function as ceRNAs by competing to bind to shared miRNAs.[32] By combining bioinformatic analyses of CircInteractome and ENCORI algorithms, we first pointed to the role of circ_0000654 as a post-transcriptional modulator of E2F3 through sponging miR-375. The high expression of miR-375 has been found in breast cancer and castration-resistant prostate cancer.[34,35] Conversely, miR-375 has been discovered to be underexpressed in colorectal cancer and liver cancer.[36,37] These findings suggest miR-375 as a diagnostic or prognostic marker for these diseases. Moreover, miR-375 is a crucial antitumor factor in many cancers, such as cervical cancer and oral squamous cell carcinoma, wherein miR-375 is downregulated in cancer tissues and cells.[38,39] Intriguingly, although miR-375 is frequently upregulated in prostate tumors, it can repress migration and invasion of prostate cancer cells.[40] These contradictory findings may be in part due to the different types of tumors and diversified tumor microenvironment. In this paper, we first demonstrated that miR-375, a potent anti-ESCC miRNA,[27,28] worked as a mediator of circ_0000654 in regulating ESCC development.

The tumor-inhibitory effect of circ_0000654 silencing was preliminarily analyzed in vivo at present. More explorations about the circ_0000654/miR-375/E2F3 ceRNA network in ESCC development in vivo will be done in further work. Previous work also uncovers the circ_0000654/miR-149-5p/IL-6 ceRNA crosstalk in regulating ESCC.[15] The two circ_0000654-mediated ceRNA networks may be two paralleled mechanisms underlying the regulation of circ_0000654 in ESCC. There may be other circ_0000654-mediated ceRNA networks that remain to be elucidated in ESCC.

To conclude, our study identifies a novel circ_0000654/miR-375/E2F3 ceRNA network for the oncogenic property of circ_0000654 in ESCC. Therefore, developing pharmacological agents that targeting circ_0000654 and its pathways may have the potential to improve ESCC outcome.

AUTHOR CONTRIBUTIONS

CL and SL conducted the experiments, designed the study and drafted the manuscript. XZ conducted the experiments

and supervised the study. YW and YL collected and analyzed the data. TW contributed the methodology and edited the manuscript. All authors reviewed the manuscript.

CONFLICT OF INTEREST

The authors declare that they have no conflict of interest.

DATA AVAILABILITY STATEMENT

The data sets used and/or analyzed during the current study are available from the corresponding author on reasonable request.

ORCID

Shumin Li https://orcid.org/0000-0002-1841-7109

REFERENCES

1. Reichenbach ZW, Murray MG, Saxena R, et al. Clinical and translational advances in esophageal squamous cell carcinoma. Adv Cancer Res. 2019;144:95–135.
2. Codipilly DC, Qin Y, Dawsey SM, Kisiel J, Topazian M, Ahlquist D, et al. Screening for esophageal squamous cell carcinoma: recent advances. Gastrointest Endosc. 2018;88:413–26.
3. Hirano H, Kato K. Systemic treatment of advanced esophageal squamous cell carcinoma: chemotherapy, molecular-targeting therapy and immunotherapy. Jpn J Clin Oncol. 2019;49:412–20.
4. Feng Q, Zhang H, Yao D, Chen WD, Wang YD. Emerging role of non-coding RNAs in esophageal squamous cell carcinoma. Int J Mol Sci. 2019;21:258.
5. Jiang C, Xu D, You Z, Xu K, Tian W. Dysregulated circRNAs and ceRNA network in esophageal squamous cell carcinoma. Front Biosci (Landmark Ed). 2019;24:277–90.
6. Ma S, Paiboonrungruan C, Yan T, Williams KP, Major MB, Chen XL. Targeted therapy of esophageal squamous cell carcinoma: the NRF2 signaling pathway as target. Ann N Y Acad Sci. 2018;1434:164–72.
7. Uno Y, Kanda M, Sato Y, et al. Expression, function, and prognostic value of MAGE-D4 protein in esophageal squamous cell carcinoma. Anticancer Res. 2019;39:6015–23.
8. Kristensen LS, Andersen MS, Stagsted LVW, Ebbesen KK, Hansen TB, Kjems J. The biogenesis, biology and characterization of circular RNAs. Nat Rev Genet. 2019;20:675–91.
9. Memczak S, Jens M, Elefsinioti A, Torti F, Krueger J, Rybak A, et al. Circular RNAs are a large class of animal RNAs with regulatory potency. Nature. 2013;495:333–8.
10. Huang H, Wei L, Qin T, Yang N, Li Z, Xu Z. Circular RNA ciRS-7 triggers the migration and invasion of esophageal squamous cell carcinoma via miR-7/KLF4 and NF-κB signals. Cancer Biol Ther. 2019;20:73–80.
11. Chen X, Jiang J, Zhao Y, Wang X, Zhang C, Zhuan L, et al. Circular RNA circNTRK2 facilitates the progression of esophageal squamous cell carcinoma through up-regulating NRIP1 expression via miR-140-3p. J Exp Clin Cancer Res. 2020;39:133.
12. Shi Y, Fang N, Li Y, Guo Z, Jiang W, He Y, et al. Circular RNA LPAR3 sponges microRNA-198 to facilitate esophageal cancer migration, invasion, and metastasis. Cancer Sci. 2020;111:2824–36.
13. Shi Y, Guo Z, Fang N, Jiang W, Fan Y, He Y, et al. hsa_circ_0006168 sponges miR-100 and regulates mTOR to promote the proliferation, migration and invasion of esophageal squamous cell carcinoma. Biomed Pharmacother. 2019;117:109151.
14. Pan Z, Lin J, Wu D, He X, Wang W, Hu X, et al. Hsa_circ_0006948 enhances cancer progression and epithelial-mesenchymal transition through the miR-490-3p/HMGA2 axis in esophageal squamous cell carcinoma. Aging (Albany NY). 2019;11:11937–54.
15. Xu Z, Tie X, Li N, Yi Z, Shen F, Zhang Y. Circular RNA hsa_circ_0000654 promotes esophageal squamous cell carcinoma progression by regulating the miR-149-5p/IL-6/STAT3 pathway. IUBMB Life. 2020;72:426–39.
16. Gao Y, Feng B, Lu L, Han S, Chu X, Chen L, et al. MiRNAs and E2F3: a complex network of reciprocal regulations in human cancers. Oncotarget. 2017;8:60624–39.
17. Feber A, Clark J, Goodwin G, Dodson AR, Smith PH, Fletcher A, et al. Amplification and overexpression of E2F3 in human bladder cancer. Oncogene. 2004;23:1627–30.
18. Manicum T, Ni F, Ye Y, Fan X, Chen BC. Prognostic values of E2F mRNA expression in human gastric cancer. Biosci Rep. 2018;38:BSR20181264.
19. Al Ahmed HA, Nada O. E2F3 transcription factor: a promising biomarker in lung cancer. Cancer Biomark. 2017;19:21–6.
20. Zhao W, Wang M, Wang C, Liu Y, Liu H, Luo S. RACGAP1 is transcriptionally regulated by E2F3, and its depletion leads to mitotic catastrophe in esophageal squamous cell carcinoma. Ann Transl Med. 2020;8:950.
21. Qian Y, Liang X, Kong P, Cheng Y, Cui H, Yan T, et al. Elevated DHODH expression promotes cell proliferation via stabilizing β-catenin in esophageal squamous cell carcinoma. Cell Death Dis. 2020;11:862.
22. Wang J, Wang Q, Gong Y, Hu Q, Zhang H, Ke S, et al. Knockdown of circRNA circ_0087378 represses the tumorigenesis and progression of esophageal squamous cell carcinoma through modulating the miR-140-3p/E2F3 Axis. Front Oncol. 2020;10:607231.
23. Sang C, Chao C, Wang M, Zhang Y, Luo G, Zhang X. Identification and validation of hub microRNAs dysregulated in esophageal squamous cell carcinoma. Aging (Albany NY). 2020;12:9807–24.
24. Zhong X, Huang G, Ma Q, Liao H, Liu C, Pu W, et al. Identification of crucial miRNAs and genes in esophageal squamous cell carcinoma by miRNA-mRNA integrated analysis. Medicine (Baltimore). 2019;98:e16269.
25. Komatsu S, Ichikawa D, Takeshita H, Konishi H, Nagata H, Hirajima S, et al. Prognostic impact of circulating miR-21 and miR-375 in plasma of patients with esophageal squamous cell carcinoma. Expert Opin Biol Ther. 2012;12(Suppl 1):S53–9.
26. Luo HS, Wu DH. Identification of miR-375 as a potential prognostic biomarker for esophageal squamous cell cancer: a bioinformatics analysis based on TCGA and meta-analysis. Pathol Res Pract. 2019;215:512–8.
27. Yi J, Jin L, Chen J, Feng B, He Z, Chen L, et al. MiR-375 suppresses invasion and metastasis by direct targeting of SHOX2 in esophageal squamous cell carcinoma. Acta Biochim Biophys Sin (Shanghai). 2017;49:159–69.
28. Xu H, Jiang J, Zhang J, Cheng L, Pan S, Li Y. MicroRNA-375 inhibits esophageal squamous cell carcinoma proliferation through direct targeting of SP1. Exp Ther Med. 2019;17:1509–16.
29. Orangi E, Motovali-Bashi M. Evaluation of miRNA-9 and miRNA-34a as potential biomarkers for diagnosis of breast cancer in Iranian women. Gene. 2019;687:272–9.
30. Hatley ME, Patrick DM, Garcia MR, Richardson JA, Bassel-Duby R, van Rooij E, et al. Modulation of K-Ras-dependent lung tumorigenesis by MicroRNA-21. Cancer Cell. 2010;18:282–93.
31. Iwakawa HO, Tomari Y. The functions of MicroRNAs: mRNA decay and translational repression. Trends Cell Biol. 2015;25:651–65.
32. Tay Y, Rinn J, Pandolfi PP. The multilayered complexity of ceRNA crosstalk and competition. Nature. 2014;505:344–52.
33. Anastasiadou E, Jacob LS, Slack FJ. Non-coding RNA networks in cancer. Nat Rev Cancer. 2018;18:5–18.
34. Tang W, Li GS, Li JD, Pan WY, Shi Q, Xiong DD, et al. The role of upregulated miR-375 expression in breast cancer: an in vitro and in silico study. Pathol Res Pract. 2020;216:152754.
35. Huang X, Yuan T, Liang M, du M, Xia S, Dittmar R, et al. Exosomal miR-1290 and miR-375 as prognostic markers in castration-resistant prostate cancer. Eur Urol. 2015;67:33–41.
36. Elshafei A, Shaker O, Abd El-Motaal O, Salman T. The expression profiling of serum miR-92a, miR-375, and miR-760 in colorectal cancer: an Egyptian study. Tumour Biol. 2017;39:1010428317705765.

37. Xie D, Yuan P, Wang D, Jin H, Chen H. Expression and prognostic significance of miR-375 and miR-221 in liver cancer. Oncol Lett. 2017;14:2305–9.
38. Jayamohan S, Kannan M, Moorthy RK, Rajasekaran N, Jung HS, Shin YK, et al. Dysregulation of miR-375/AEG-1 Axis by human papillomavirus 16/18-E6/E7 promotes cellular proliferation, migration, and invasion in cervical cancer. Front Oncol. 2019;9:847.
39. Wu Y, Sun X, Song B, Qiu X, Zhao J. MiR-375/SLC7A11 axis regulates oral squamous cell carcinoma proliferation and invasion. Cancer Med. 2017;6:1686–97.
40. Selth LA, Das R, Townley SL, Coutinho I, Hanson AR, Centenera MM, et al. A ZEB1-miR-375-YAP1 pathway regulates epithelial plasticity in prostate cancer. Oncogene. 2017;36:24–34.

SUPPORTING INFORMATION

Additional supporting information can be found online in the Supporting Information section at the end of this article.

How to cite this article: Luo C, Zhao X, Wang Y, Li Y, Wang T, Li S. A novel circ_0000654/miR-375/E2F3 ceRNA network in esophageal squamous cell carcinoma. Thorac Cancer. 2022;13(15):2223–34. https://doi.org/10.1111/1759-7714.14550